

ADA 952010

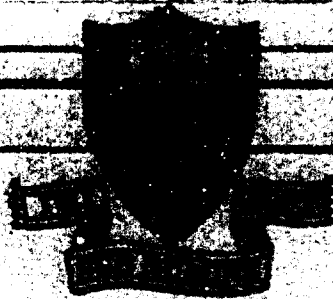
DEC 5 1965
APR 1 1965
452-5125
copy 2

①

AN EXPERIMENTAL INVESTIGATION
 OF LAMINAR HYPERSONIC CAVITY FLOWS
 Part II: Heat-Transfer and Recovery
 Factor Measurements

K. M. Nicoll
 Princeton University

Report 655 February 1963



Reproduced From
Best Available Copy

DTIC
ELECTE
SEP 8 1963
S D

PRINCETON UNIVERSITY
 THE JAMES H. JOHNSON
 LIBRARY CENTER

AN EXPERIMENTAL INVESTIGATION
OF LAMINAR HYPERSONIC CAVITY FLOWS
Part II: Heat-Transfer and Recovery
Factor Measurements

K. M. Nicoll
Princeton University

Report 655

February 1963

Contract AF 33(616)-7629
Project No. 7064
Task No. 70169

Aeronautical Research Laboratory
Office of Aerospace Research
United States Air Force
Wright-Patterson Air Force Base, Ohio

DTIC
ELECTE
SEP 8 1983
S D

B

DISTRIBUTION STATEMENT A

Approved for public release
Distribution Unlimited

FOREWARD

The present study is part of a program of theoretical and experimental research on hypersonic flow being conducted by the Gas Dynamics Laboratory of the Department of Aeronautical Engineering at the James Forrestal Research Center, Princeton University. This study is sponsored by the Aeronautical Research Laboratory, Wright Air Development Division, under Contract AF 33(616)-7629, "Research on Boundary Layer Characteristics in the Presence of Pressure Gradients at Hypersonic Speeds", with Capt. W. W. Wells and Col. A. Boreske as consecutive project officers.



Accession For	
NTIS GRA&I	<input checked="" type="checkbox"/>
DTIC TAB	<input type="checkbox"/>
Unannounced	<input type="checkbox"/>
Justification	
PER - LETTER	
By 1963	
Distribution/	
Availability Codes	
Dist	Avail and/or Special
A	

UNANNOUNCED

TABLE OF CONTENTS

I.	INTRODUCTION.	1
II.	EXPERIMENTAL EQUIPMENT AND TECHNIQUES . . .	1
III.	RESULTS OF EXPERIMENTS.	6
IV.	DISCUSSION.	11
V.	CONCLUDING REMARKS.	17
	REFERENCES.	19

ABSTRACT

An experimental investigation has been made of the recovery factor and heat-transfer distributions on a set of cone-models incorporating annular cavities. This study is the second part of a two-part program. The first section contained measurements of the pressure distributions.

The cone-surface Mach number was 6.5, the free-stream Mach number was 11.2, and all experiments were carried out in helium. All cavity flows were "open", and all heat-transfer tests were in the laminar regime.

The results show that the recovery factor in laminar, hypersonic cavity flow is almost constant within the cavity and downstream of reattachment, and is very close to the laminar attached-flow value. In the immediate vicinity of reattachment, the recovery factor is slightly higher than this value. (Less than 5%).

The lowest values of the heat-transfer coefficient are found on the cavity floors, where a minimum of about ten to twenty percent of the attached-flow value is reached. The highest values of the heat-transfer coefficient are in the immediate vicinity of reattachment. An average reattachment heat-transfer coefficient of about three times the basic cone heat-transfer coefficient was measured on one cavity model.

On one model, the integrated heat-transfer in the separated-flow region was evaluated, and was found to be about 55% of the corresponding attached-flow value, in agreement with Chapman's theory.

NOTATION

A	External Area of model surface
C_p	Specific Heat at Constant pressure
D	Maximum depth of cavity
h	Local heat-transfer coefficient
L	Length of cavity, $x_R - x_S$
L_1	Length of model surface before separation shoulder, measured along slant side of cone
\tilde{L}	Swept length of cavity, \tilde{x}_S
M	Mach number
P	Pressure
Pr	Prandtl number
Q	Total heat transfer rate per unit time
q	Local heat transfer rate per unit area per unit time
r	Local recovery factor, $\frac{T_{aw} - T_o}{T_o - T_o}$
Re	Reynolds number based on fluid properties at the edge of the boundary layer on the basic cone
St	Stanton number, defined as $\frac{h}{\rho_o C_p u_o}$
t	Time
T	Absolute temperature
u	Velocity in x direction
x	Distance measured from nose along slant side of basic cone
\tilde{x}	Distance measured along wetted cavity surface from reattachment shoulder

\bar{x} defined as $(x - x_R)$ on surfaces downstream of cavity
 δ Boundary Layer thickness
 β Cone half-angle
 ρ Mass density
 μ Viscosity coefficient

Subscripts:

aw Adiabatic wall conditions
c, cone Values on basic cone
cav Value on cavity model
e Conditions at edge of boundary layer or shear layer
i Initial conditions before test
t = 0+ Instant of flow start
R Reattachment shoulder
S Separation shoulder
X Crossing-point
 ∞ Free-stream conditions
o Isentropic stagnation conditions
w Model wall conditions

INTRODUCTION

The present work is the second part of a report on an experimental study of laminar hypersonic cavity flows. In the first section, (reference (1)), the general program was described, and the measurements of the pressure distributions on a series of 20° cone-models incorporating annular cavities were reported. In this, the second section, measurements of the distribution of local recovery factor and local heat-transfer coefficient on models of the same geometry are presented. As in (reference (1)), the free-stream Mach number was about 11, and the cone-surface Mach number was 6.5. The test gas was helium, with a stagnation temperature of room temperature.

EXPERIMENTAL EQUIPMENT AND TECHNIQUES

As with the pressure studies, all tests were made in the 3" helium hypersonic tunnel of the Gas Dynamics Laboratory at Princeton University. Experiments were carried out at three levels of stagnation pressure - 400, 700 and 1,000 psia. The heat-transfer and recovery-factor models had the same geometry as the pressure models, (see reference (1)), with the exception that the $1/16$ " deep cavity models were omitted. In other words, cavity geometries used for the present work had lengths of $5/16$ ", $5/8$ " and $1-1/4$ ", and depths of $3/32$ " and $1/8$ ". A heat-transfer model for the $5/8$ " x $1/8$ " single-arc geometry was also built, making a total of seven configurations. As before, the length of the model before the separation point was kept constant at $1-1/4$ " (measured along slant side of cone). All models incorporated the 0.005" standard nose, and were made with four pressure taps spaced 90° apart at a single axial station

for model alignment while the tunnel was running. Sample models are shown in figure (1).

The heat-transfer measurements were made using the transient "thin-wall" technique, and a detailed description of the use of this technique in hypersonic separated flows is given in reference (2). Since this reference contains all relevant information on the experimental method used for the present work, only a brief outline will be given here.

The transient method uses a model with a thin metal skin, instrumented with thermocouples. At the beginning of a test, the model is isothermal at a particular initial wall temperature. The flow is then started suddenly, and the thermocouple output recorded on fast-response continuous-record potentiometers as the model cools towards recovery temperature. The initial gradient of the resultant temperature-time trace at each model station is a measure of the heat-transfer rate at that point. In addition to this method of measuring the initial heat-transfer rate, some of the data from the present experiments were analysed using the first two seconds of each temperature-time trace from points in the cavity, and applying the full conduction equation for the temperature history in the skin. In the present report, this is called the "conduction method" of data reduction, and results obtained in this way are denoted by shaded symbols in the figures.

Experiments were carried out at several levels of initial wall temperature using infrared heat-lamps to raise the model temperature before a run. The final results were obtained by plotting the initial temperature gradient against initial wall temperature, together with independent measurements of the adiabatic wall temperature, and using the slope of

the resultant straight line as the final measure of the heat-transfer coefficient. (The modified Newtonian Law was found to hold throughout.) The recovery temperature distribution was measured using the thin-skin metal models by simply running the tunnel for about seven to ten minutes and recording the final thermocouple outputs. For the normalising cone and for one cavity configuration, special recovery-factor models were made from an insulating material, (plexiglass), and instrumented with surface thermocouples. The results from these models were virtually identical to the data obtained from the corresponding metal models.

In reference (2), concern was expressed about the time taken for the steady-state distribution of temperature and velocity in the cavities to be established. (For the use of the transient technique to be valid, this must occur virtually instantaneously.) Since a true steady-state measurement technique was not available in the laboratory, a form of the transient method was developed to approximate the steady state technique. This method was used to spot-check the conventional transient measurements.

The method is basically the insulated-mass technique described by Westkaemper in reference (3). A model was built which corresponded to the geometry of the $L = 1\text{-}1/4"$, $D = 3/32"$ cavity model. Most of the model was made of solid copper, but at the mid-point of the cavity a thin (0.01") steel annulus was mounted. The steel ring was insulated from the copper part of the model with plexiglass washers, and the copper model was insulated from the supporting sting with a nylon sleeve. Thermocouples were mounted in the steel annulus, and in the copper body. The model is shown in figure (1). (Lowest model.)

A test on this model was begun in the normal way. The model was

isothermal at the beginning of the test, and the tunnel was started suddenly. Figure (2) is a tracing of the temperature-time history of the steel annulus during a typical run, superimposed on that of the copper section of the model. At A the tunnel starts; the heavy copper model falls slowly in temperature as it is cooled by the stream. The steel section, being much lighter, and having therefore a very low heat capacity, cools more quickly. At point B, infrared heat lamps are turned on. These give a higher heat input than the cooling power of the flow in the cavity, and the temperature of the steel section rises. (The steel was painted matt black to increase its absorption coefficient.) The heat lamps have little effect on the copper body because of its large thermal capacity, and because the heat transfer rate from the stream is so high outside the cavity. At C the heat lamps are turned off, and the steel annulus again quickly cools. At X, the steel has cooled to the same temperature as the copper body, and continues to cool past this temperature.

Now, if the thermal conductivity of the copper is high enough, the entire model will be substantially isothermal at point X. As a result, the temperature gradient of the steel annulus at this point will give a measure of the heat transfer rate in the mid-point of the cavity associated with an isothermal model temperature of T_w_x . The crossing-point X occurs some time after the tunnel was started (about 15 to 30 seconds for various runs), and the measurement at this point should be clear of any starting transients.

The method is probably not as accurate as the normal transient technique, because the thermal conductivity of the copper is finite, and

the model is not therefore strictly isothermal. However, it is felt that this technique should be a good check on the thin-skin method.

In the data from the thin-skin heat transfer models, the results were obtained using the correct skin thickness for most of the configurations tested. The models were cut apart after testing and the wall thickness at each measuring station measured accurately. However, this was not done for the 5/16" x 1/8" and 1-1/4" x 1/8" cavity models, which are being reserved for possible future tests. For these models, the data were reduced using the machinist's estimate of 0.01" wall thickness throughout. Experience with this type of model has shown that this estimate is correct to about ± 0.0005 ", which might result in a possible $\pm 5\%$ error in heat transfer rate.

None of the models described above could be used to measure recovery factor and heat-transfer rate in the immediate vicinity of reattachment. (Specifically, in the region considered by Chung and Viegas in reference (4). It is shown in this reference that the significant length bounding the "reattachment" region in a cavity flow is of the order of the mixing layer thickness). Accordingly, two additional models were constructed for the normal $L = 5/8$ ", $D = 1/8$ " cavity geometry which measured the average recovery factor and heat-transfer rate in the reattachment region. These models are shown in figure (3).

The recovery factor model was made of plexiglass, and had an annular circuit-paint measuring element at the reattachment shoulder. The circuit-paint band was 0.02" wide, and was recessed into the plexiglass surface and machined flush. Thermocouples were installed at 90° intervals around the circumference.

The heat-transfer model was made of brass, and had a copper ring of approximately square cross-section mounted in a plexiglass spacer at the reattachment corner. The cross-section of the copper ring was 0.03" on a side, and four thermocouples were again installed around the circumference. The heat-transfer rate was measured by recording the temperature-time variation of the copper ring during a run. The details of this method are virtually identical to the thin-skin technique.

RESULTS OF EXPERIMENTS

MEASUREMENTS OF RECOVERY FACTOR AND HEAT-TRANSFER COEFFICIENT ON THE BASIC CONE

The recovery-factor measurements on the 20° cone are given in figure (4), as local recovery factor against cone Reynolds number. The heat-transfer results are given in figure (5), as Stanton number against cone Reynolds number. All fluid properties are evaluated at the edge of the cone boundary layer. The theoretical values for recovery factor and heat-transfer coefficient in laminar flow are taken from reference (5).

The recovery factor data in figure (4) indicate that natural transition occurred on the cone at a Reynolds number of about two million. In reducing the heat-transfer results, the laminar recovery-factor value of 0.815 was used throughout, and the data of figure (5) are therefore unreliable above $Re \sim 2 \times 10^6$. (The heat-transfer coefficient results do not show a rise at high Reynolds numbers, which may indicate either that the increase is smothered by the use of a constant recovery factor in reducing the data, or that the different experimental conditions in the heat-transfer tests result in a somewhat higher transition Reynolds number.)

In any event, only the laminar data were of interest in the present

Investigation, and these data were used to normalise the cavity-model heat-transfer rates. The cone recovery-factor results are presented to indicate the range of purely laminar flow, and these results were used in conjunction with the transition evidence of the first part of this report to limit the experiments to a Reynolds number below two million.

RECOVERY-FACTOR MEASUREMENTS ON THE CAVITY MODELS

These results are presented in figures (6) through (9). The results are for laminar cavity flow only, and the possible stagnation pressure of the tests therefore descends as the cavity length increases. For the $L = 5/16$ " cavity models stagnation pressures of 400, 700 and 1,000 psia could be used, but for the $L = 1-1/4$ " cavity models, only tests at $P_0 = 400$ psia were always laminar. All the results given were obtained using the thin-skin heat-transfer models, with the exception of the $5/8$ " x $1/8$ " cavity geometry, for which both plexiglass and metal models were tested.

The results of all tests show that the recovery factor for the laminar cavity flows is little different from that of the basic model with attached boundary layer. For the case of the $5/8$ " x $1/8$ " cavity geometry, the recovery factor in the immediate vicinity of reattachment was measured using the special model shown in figure (3). The results are included in figure (7), and it is seen that the recovery factor at reattachment is of the order of 5% higher than elsewhere. The reattachment heat-transfer model for this geometry was also used to obtain recovery factor measurements, by simply recording the final temperature of the copper ring after about seven minutes running time. The reattachment zone recovery factor measurements using the two models were identical. This is an indication that the average measurements describe the

true reattachment point value quite accurately, since the measuring area for the heat-transfer model was three times as large as for the recovery-factor model.

Increasing the value of δ_s/D is seen to cause a slight reduction in the recovery factor level for the present experiments. This is probable due to the effect of the finite initial boundary layer thickness. Increasing this thickness would lower the velocity on the dividing streamline, and hence lower the kinetic impact pressure.

MEASUREMENTS OF HEAT-TRANSFER COEFFICIENT ON THE CAVITY MODELS

The local heat-transfer coefficient h is defined in the usual way using the modified Newtonian Law, namely

$$q = h (T_w - T_{aw})$$

For the thin-wall measuring technique, this can be written

$$\rho_w c_w \frac{V}{A_w} \left(\frac{\partial T_w}{\partial t} \right)_{t=0+} = h (T_{w1} - T_{aw})$$

where the quantities on the left-hand side are for a wall element at a particular model station. $(V/A)_w$ is the volume to external area ratio, and is approximately equal to the skin thickness. (The correct ratio is calculated from the particular model geometry.)

The results of the experiments are given in figures (10) through (16), as local heat-transfer coefficient normalised by the equivalent cone value, plotted against distance from the model nose along the slant side of the basic cone. All results are for laminar flow in the cavity.

The heat-transfer results from each model configuration show the same general characteristics. The heat transfer is greatest at reattachment, and falls off both upstream and downstream of this point. In the cavity, the heat transfer coefficient falls to about 10 to 20% of the basic-cone value and then rises again near the separation shoulder. Downstream of reattachment, the heat-transfer coefficient falls to the cone value within one cavity length, and in most cases falls below the cone value further downstream.

For the 5/8" x 1/8" cavity geometry, measurements of the average heat-transfer rate in the reattachment region were made using the copper-ring model shown in figure (3). When the results were reduced using the previously measured values of the recovery factor in the vicinity of reattachment, the following values of h/h_{cone} were obtained.

<u>Stagnation pressure (psia)</u>	<u>h/h_{cone}</u>
400	2.63
700	2.90

These values fit the trend of the thin-wall data for the 5/8" x 1/8" model.

Changing the boundary-layer thickness at separation (i.e. varying the stagnation pressure) was found to have little effect on the distribution of h/h_{cone} in the cavities. However, it should be remembered that δ_s was varied in the present experiments only by a factor of about 1-1/2.

Downstream of the cavity, increase of δ_s/D was found to lower the final level of h/h_{cone} . On the two models for which tests were made at $p_0 = 1000$ psia, there are indications of transition downstream of the cavities.

The measurements made of the heat transfer rate in the centre of the cavity on the model with $L = 1-1/4"$, $D = 3/32"$ using the insulated-mass model were found to agree very well with the measurements made using the thin-wall method. (See Figure (15).) This is a definite indication that no starting transients exist on the present configurations, and supports the analysis of reference (2).

The results of the heat transfer measurements on the single-arc cavity model (figure (16)) are little different from those on the models with the normal cavity geometry used in the present work. The floor heat transfer rate is a little higher than on the other models carrying $5/8"$ long cavities, but otherwise the distribution of h/h_{cone} is similar. At the $X = 2"$ station on the single-arc model, the measured heat-transfer rate does not fall on a smooth curve through the rest of the data, but it is not known whether this has any significance or not. The thermocouples on this model were calibrated and tested very carefully, and no reason was found for rejecting the data from the thermocouple at the $X = 2"$ station.

In figure (17), the cavity data from all models at all stagnation pressures are plotted on the same scales for comparison purposes. The abscissa is \tilde{x}/\tilde{L} where \tilde{x} is the distance measured along the cavity surface from the reattachment point. It is seen that the h/h_{cone} distribution varies roughly with the inverse of \tilde{x}/\tilde{L} , although the data from the reattachment corner follow the inverse half power more closely. This figure also shows that, in general, the deeper cavities have slightly lower values of floor heat-transfer coefficient.

Some preliminary heat-transfer results from the first model built for the present program were published some time ago in reference (6).

These results have since been found to be in error and are to be replaced by the present data. The reasons for this correction form the subject of reference (2).

DISCUSSION

As mentioned in the previous section of this report, there do not appear to be any other investigations of laminar, hypersonic cavity flow available with which to compare the present work. The most similar experiments are those of Larson in reference (7), which were carried out at Mach numbers from 0.3 to 4.0. The present heat-transfer results are in good agreement with the laminar measurements of Larson. Larson was primarily interested in the average heat transfer rate, but his experimental method allowed an estimate of the local variations in heat transfer coefficient. These latter results show the same high heat transfer at reattachment, and low heat-transfer on the cavity floor as do the present measurements.

The local variation in heat transfer coefficient along the cavity surfaces is qualitatively what would be expected on physical grounds. The reattachment point is a stagnation point of the fluid passing along the dividing streamline and the heat transfer coefficient is high at this point. As the fluid recirculates around the cavity in contact with the wall surfaces, it gradually loses its capacity to transfer heat, as the layers of fluid near the wall more closely approach the wall temperature. In addition, if one thinks of a boundary layer growing in an upstream direction from the reattachment point (see reference (4)), the effective "boundary layer thickness" becomes larger as the reversed flow near the wall passes under the core of slowly moving fluid around the $u = 0$ locus.

On the surfaces downstream of reattachment, the heat transfer coefficient eventually falls below the pure-cone value, provided the flow remains laminar. This is because the boundary layer is thicker on the cavity model downstream of reattachment than on the basic cone because of the rapid shear layer growth. (The laminar shear layer grows about three times as quickly as a laminar boundary layer.)

For the 5/8" x 1/8" cavity model, heat-transfer measurements were made in the immediate vicinity of reattachment. These results, combined with the measurements made outside the reattachment region with the "thin-wall" technique, were used to calculate the overall heat-transfer rate in the separated region on this model. The measuring element on the copper-ring model used to measure the reattachment heat transfer rate had two exposed faces of virtually equal area, one forming part of the cavity surface, the other on the cone surface downstream of the cavity. In calculating the total cavity heat transfer, it was assumed that the heat-transfer to the copper ring was divided equally between its two faces. The validity of this assumption was checked in the following way.

The measurements made outside the reattachment region using the thin-wall 5/8" x 1/8" model were analyzed, and it was found that the data were well represented by the laws

$$h_{cav} = \text{const.} \times (\bar{x})^{-1/4}$$

In the cavity near reattachment, and

$$h_{cav} = \text{const.} \times (\bar{x})^{-1/4}$$

on the conical surfaces of the model downstream of reattachment, for a particular stagnation pressure. The constants were determined from the

thin-wall model results. It was found that if these relationships were assumed to hold into the reattachment region, and the average heat-transfer rate in the region spanned by the copper ring were calculated, the results agreed very well with the values actually measured by the copper-ring model. In addition, the heat-transfer distribution from the above variations showed that an equal division of heat transfer between the upstream and downstream faces of the ring was a valid assumption.

Using this assumption to obtain the average heat-transfer rate on the reattachment face, the total heat-transfer rate in the cavity was calculated by integrating the local variation of the heat-transfer coefficient along the cavity surface. It was found that any reasonable assumption for the local variation of heat-transfer coefficient in the reattachment region which gave the correct average value would yield virtually the same total cavity heat-transfer rate after integration. The value of the adiabatic wall temperature was assumed to be constant and equal to the laminar cone value. (The experimental results show that this is a reasonable assumption.) This enabled the total cavity heat-transfer rate to be compared with the corresponding value for an attached boundary layer between the same model stations by comparing the corresponding overall heat transfer coefficients.

In this way, the comparison parameter H was evaluated, where H is defined by

$$H = \frac{\bar{q}_{cav}}{\bar{q}_{cone}} = \frac{\int_0^{L_1+L} \frac{h_{cav}}{h_{cone}} h_{cone} \frac{dA_{cav}}{dx} dx}{\int_{L_1}^{L_1+L} h_{cone} \frac{dA_{cone}}{dx} dx}$$

This parameter H is comparable to Chapman's parameter " $\bar{q}_w/(\bar{q}_w)_{bl}$ " in reference (8).

The values of H calculated for the two stagnation pressures used for the 5/8" x 1/8" model were as follows:

$p_o(\text{psia})$	$H = \bar{Q}_{cav}/\bar{Q}_{cone}$
400	0.546
700	0.544

The theoretical value of H from Chapman's theory in reference (8) is 0.55, for a Prandtl number corresponding to helium. Excellent agreement with Chapman's result is evident. Larson, in reference (7), working with cavity flows at supersonic Mach numbers in air, also obtained virtually exact agreement with Chapman's theory. In view of the rather extreme assumptions involved in the derivation of Chapman's solution, it is surprising that the experimental agreement should be so good. However, although the cavity flows studied by Larson and by the present author were quite different in geometrical configuration, both sets of experiments were carried out with cavities which had comparatively small length-depth ratios. It remains to be determined whether Chapman's theory can be applied to much longer (but still "open") laminar cavity flows.

In addition to the above, the total heat-transfer to the cavity model over a surface composed of the cavity plus one cavity length downstream of reattachment was calculated, and compared with the corresponding heat-transfer to a conical surface between the same stations. (The local heat-transfer rate on the cavity model recovers to the cone value within about one cavity length downstream of R_1 .) This quantity is a measure of the total advantage in heat-transfer reduction obtained by replacing an attached boundary layer with a cavity-type separated layer. It was

found that the overall heat-transfer rate was reduced by about 10%. In other words, most of the reduction in heat-transfer rate in the cavity was countered by an increased heat-transfer on the downstream surfaces.

In reference (9), Charwat et al published results of experiments on turbulent cavity flows at supersonic Mach number. In these experiments it was found that unsteady mass exchange was taking place between the cavity and the external stream. In the present work, no evidence of mass shedding from the cavity was ever obtained in the laminar regime.

In reference (4), Chung and Viegas present a theory for the pressure and heat-transfer distributions in the reattachment zone of a cavity-type separated flow. In this work, the authors first consider the flow near the reattachment point to be inviscid and incompressible, but rotational. They solve for the stream function in closed form, evaluating the vorticity from an incoming velocity distribution obtained by fitting an exponential to the mixing layer profiles of Chapman. The solution is then used as the external condition for a boundary layer starting at the reattachment point.

The analysis yields a characteristic length in which virtually all of the pressure decay from the reattachment stagnation point occurs. This length is of the order of the mixing layer thickness. When the analysis of Chung and Viegas was applied to the experimental conditions of the present work, it was found that complete pressure decay should be accomplished about 10% of the cavity depth below the reattachment shoulder. Some recent detailed measurements made by the present author of the pressure distribution in the immediate vicinity of reattachment on the 5/8" x 1/8" cavity configuration show that the pressure decay distance given by the theory of Chung and Viegas is much too small. In addition, when the heat-transfer results of the present investigation were compared with the

prediction of reference (4), considerable disagreement was found. The average heat-transfer rate in the vicinity of reattachment on the $5/8" \times 1/8"$ copper-ring model was found to be about half of that given by the theory of Chung and Viegas.

There are a number of possible reasons for this discrepancy between the present experimental results and the analysis of reference (4). Chung and Viegas state that their approximate heat-transfer analysis is "based on the theory of a highly cooled boundary layer" but they do not give sufficient information to determine whether the analysis can be applied to cases in which the wall temperature is of the same order as the adiabatic value (as in the present experiments). In addition, the accuracy of the present experimental results is limited by the assumption that the heat-transfer rate to the measuring element on the copper-ring model is split equally between its two faces. However, there is yet another possibility. Chung and Viegas make the a priori assumption that the fluid on the dividing streamline reattaches at a right angle to the cavity wall. (The model angle at R is taken as 90° as in the present basic experimental configuration.) It is difficult to see how this assumption is justified on a physical basis. One might expect intuitively that the angle should be closer to the potential solution for uniform flow approaching a right-angled corner, which would be $3\pi/4$. If the true angle of reattachment were larger than that assumed by Chung and Viegas, the result would be an increase in the size of the reattachment zone and a drop in heat-transfer. This would bring the theoretical result more in line with the present experiments.

CONCLUDING REMARKS

The present investigation gives results of measurements of the local distribution of recovery factor and heat-transfer coefficient in laminar, hypersonic cavity flows. The free stream Mach number was 11.2 and the test gas was helium. The cavity-models were based on a 20° cone, and the cone surface Mach number was about 6.5. Wall temperatures equal to, and slightly greater than the free-stream stagnation temperature were used.

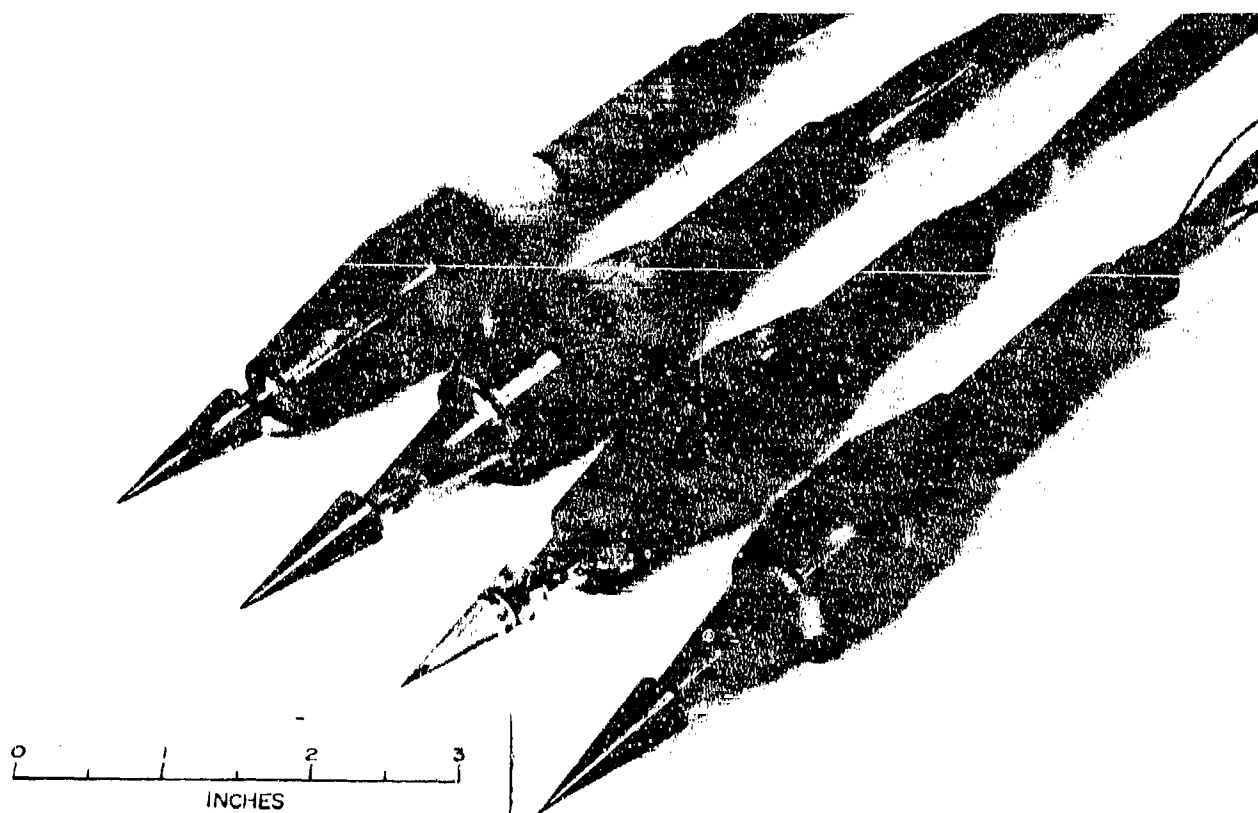
The principal results of the experiments may be summarised as follows:

- (1) The recovery factor on the cavity models was found to be very close to the value obtained in laminar flow on the basic cone with an attached boundary layer. At reattachment, the recovery factor was a little higher than elsewhere (less than 5%).
- (2) For all models tested, the heat transfer coefficient was found to be a maximum in the reattachment region, and to fall off both upstream and downstream of this point. On one model, the average heat transfer coefficient in the immediate vicinity of reattachment was measured, and was found to be about 2-1/2 to 3 times as high as the corresponding cone value.
- (3) The heat-transfer coefficient was lowest on the cavity floors, reaching a minimum of about 10 to 20% of the attached value.
- (4) The value of h_{cav}/h_{cone} more than one cavity length of reattachment was nearly always slightly less than one.

- (5) On the configuration for which sufficient measurements were made to calculate the overall heat-transfer rate to the cavity, excellent agreement was obtained with Chapman's theoretical value; i.e. the total heat-transfer rate in the region of separated flow was found to be about 55% of the corresponding attached-flow value.
- (6) On the configuration mentioned in (5), it was found that the substantial reduction in heat-transfer rate due to the presence of the separated-flow region was largely countered by the increased heat-transfer to the surfaces downstream. For the cavity plus one cavity length downstream of reattachment, the total heat transfer was about 10% lower than for a corresponding attached flow. It must be stressed that this conclusion and conclusion (5) refer to a cavity configuration with $L/D = 5$, and the possibility remains that the integrated heat transfer rates may be dependent on the cavity length-depth ratio.
- (7) The theory of Chung and Viegas was found to overestimate the average heat transfer rate in the immediate vicinity of cavity reattachment by a factor of two.

BIBLIOGRAPHY

1. Nicoll, K. M.: An Experimental Investigation of Laminar, Hypersonic Cavity Flows. Part I: Pressure Measurements. PUAED 638, December 1962; also published as ARL 63-73.
2. Nicoll, K. M.: The Use of the Transient "Thin-Wall" Technique in Measuring Heat Transfer Rates in Hypersonic Separated Flows. PUAED 628, July 1962; also published as ARL 63-72.
3. Westkaemper, J. C.: An Experimental Evaluation of the Insulated-Mass Technique of Measuring Heat Transfer at High Velocities. D.R.L.-439, Univ. of Texas, March 1959.
4. Chung, P.M. and Viegas, J.R.: Heat Transfer at the Reattachment Zone of Separated Laminar Boundary Layers. NASA TN D-1072, September 1961.
5. Nicoll, K. M.: Investigation of the Laminar Boundary Layer on a Flat Plate in Helium, Using the Crocco Method. PUAED 590, December 1961; also published as ARL 62-345.
6. Bogdonoff, S. M. and Vas, I. L.: Some Experiments on Hypersonic Separated Flows. ARS Journal, October 1962.
7. Larson, H. K.: Heat Transfer in Separated Flows. IAS Report 59-27, January 1959.
8. Chapman, D. R.: A Theoretical Analysis of Heat Transfer in Regions of Separated Flow. NACA TN 3792, October 1956.
9. Charwat, A. F.; Dewey, C. F.; Roes, J. N. and Hiltz, J. A.: An Investigation of Separated Flows. JASS, June and July 1961.



XII D4-1

Figure 1. Sample heat-transfer and recovery-factor models

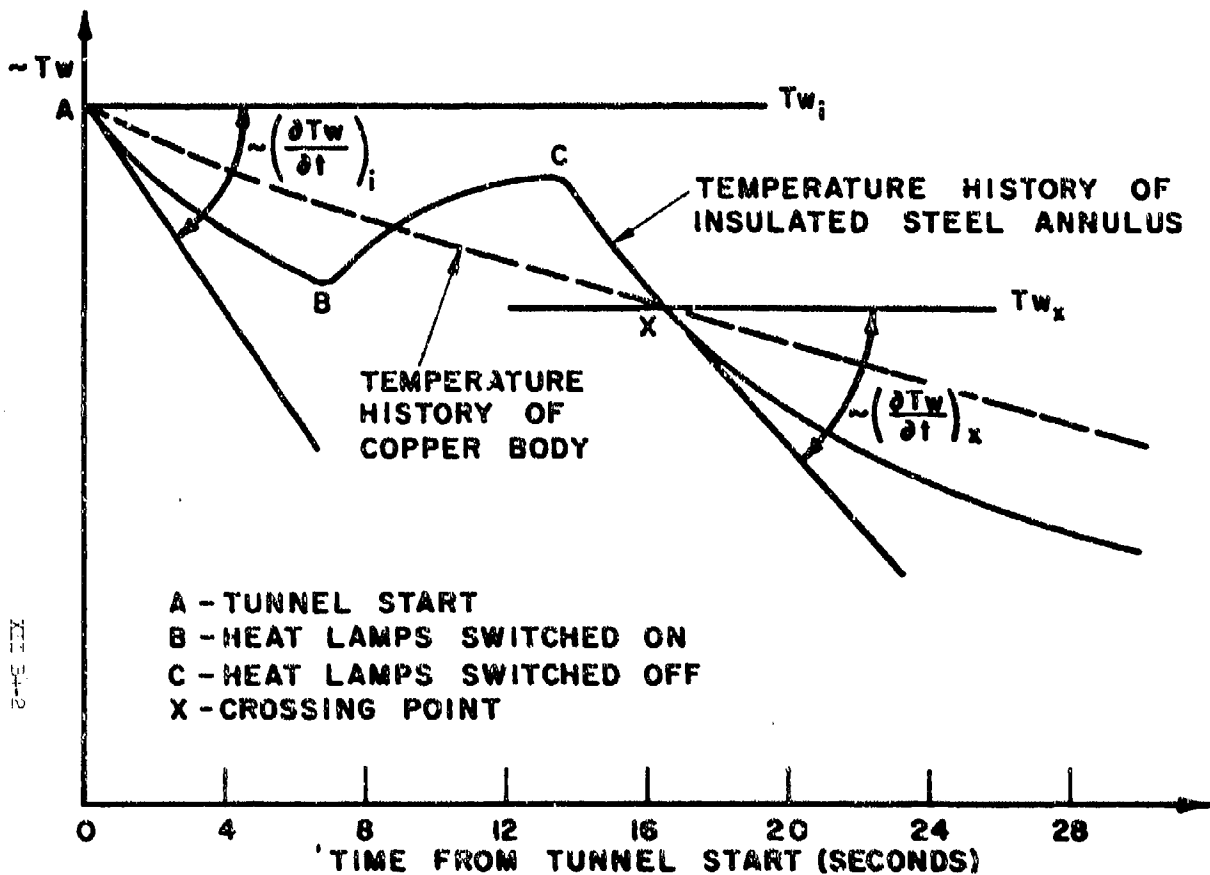
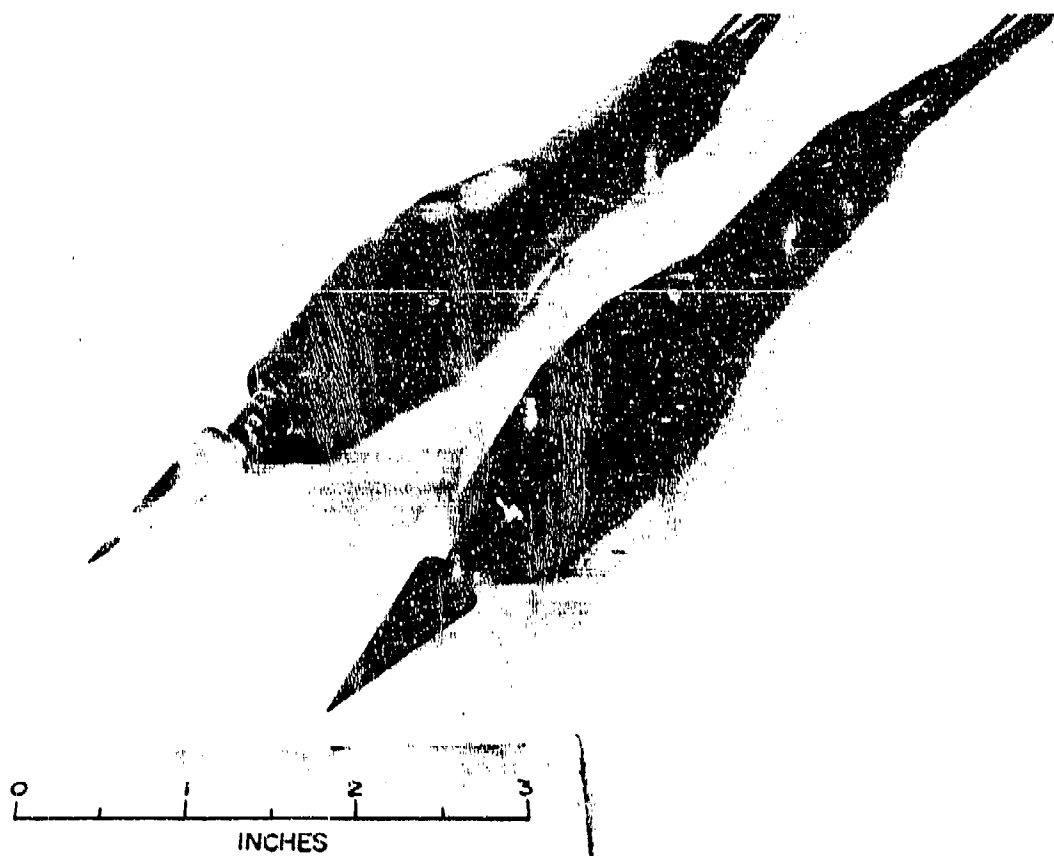


Figure 2. Sample data from insulated-mass model,
 $L = 1\frac{1}{4}"$, $D = 3/32"$



XII 04-5
Figure 3. Reattachment recovery-factor
and heat-transfer models

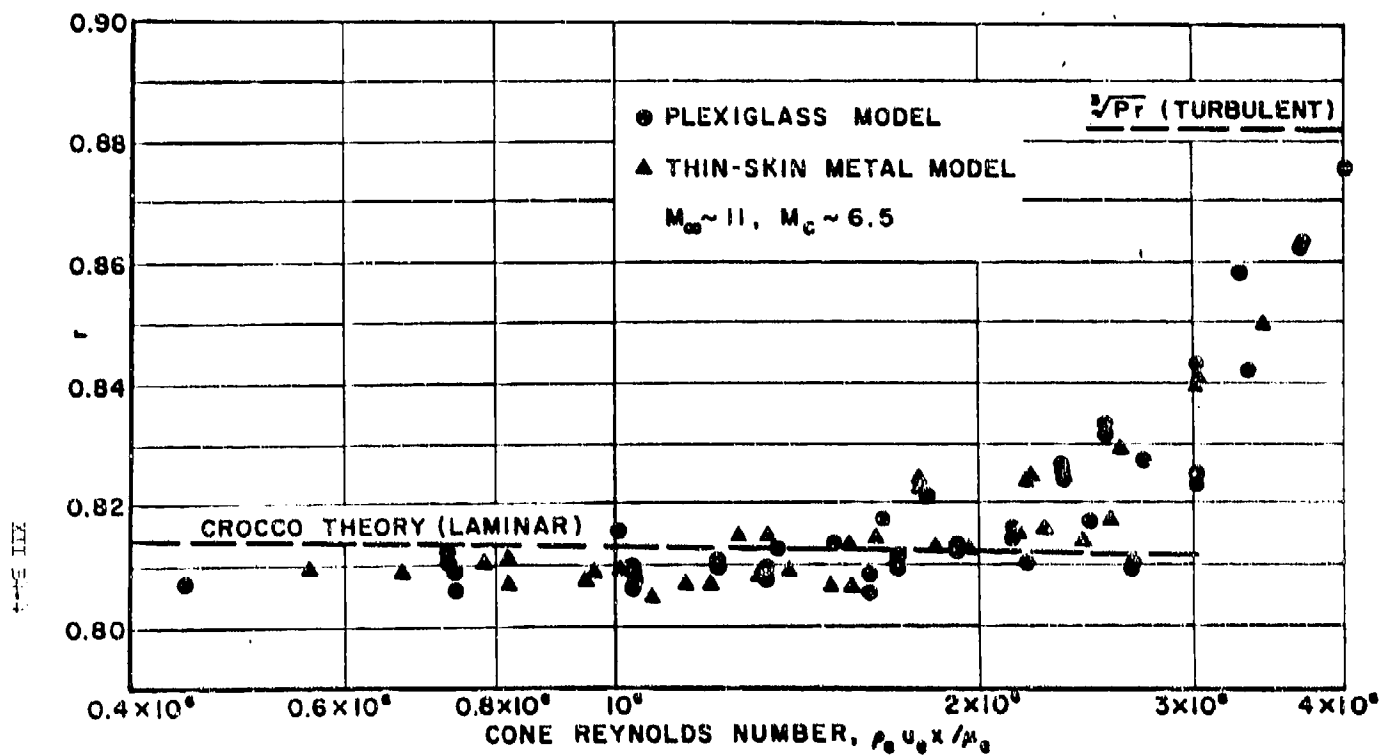


Figure 4. Local recovery factor on pure-cone)
(20° total angle)

XII 5-5

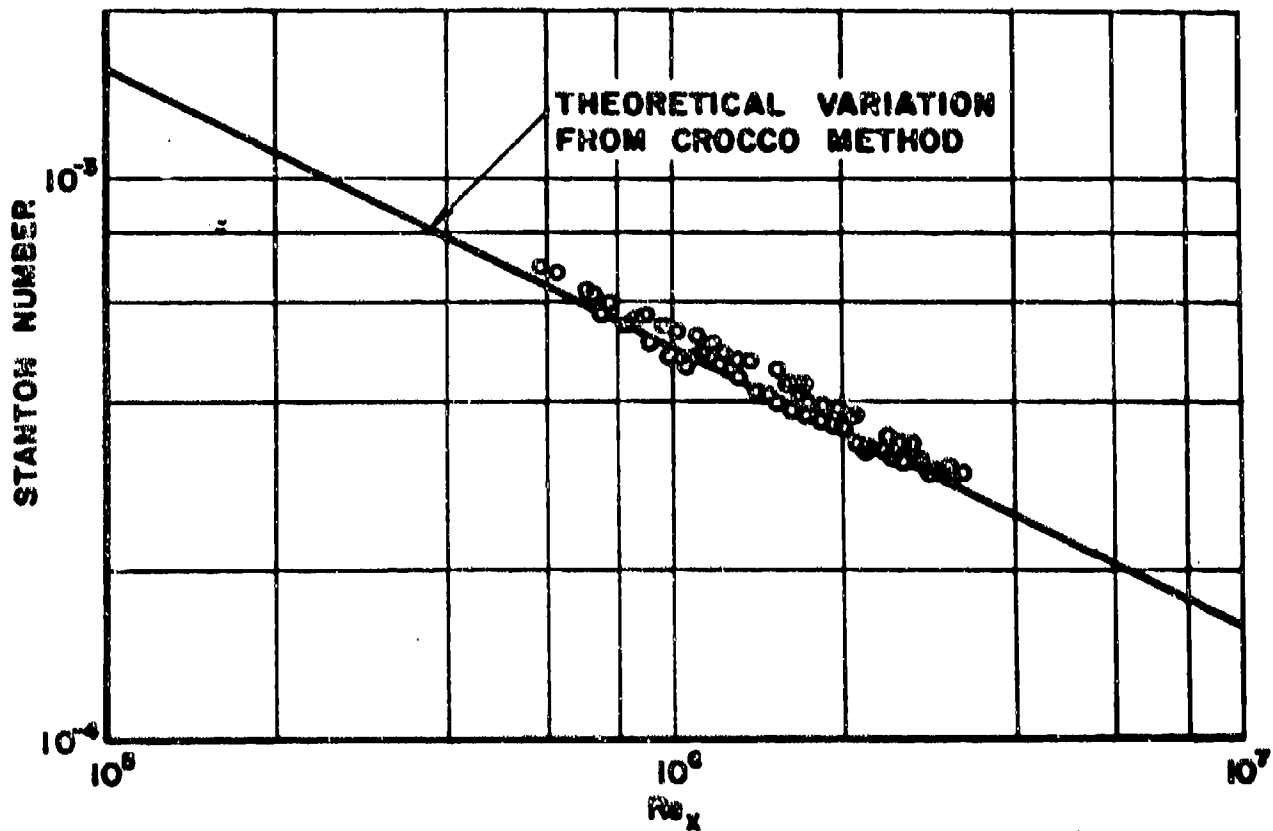


Figure 5. Experimental heat-transfer results on 20° total angle cone at $M_\infty \sim 11$

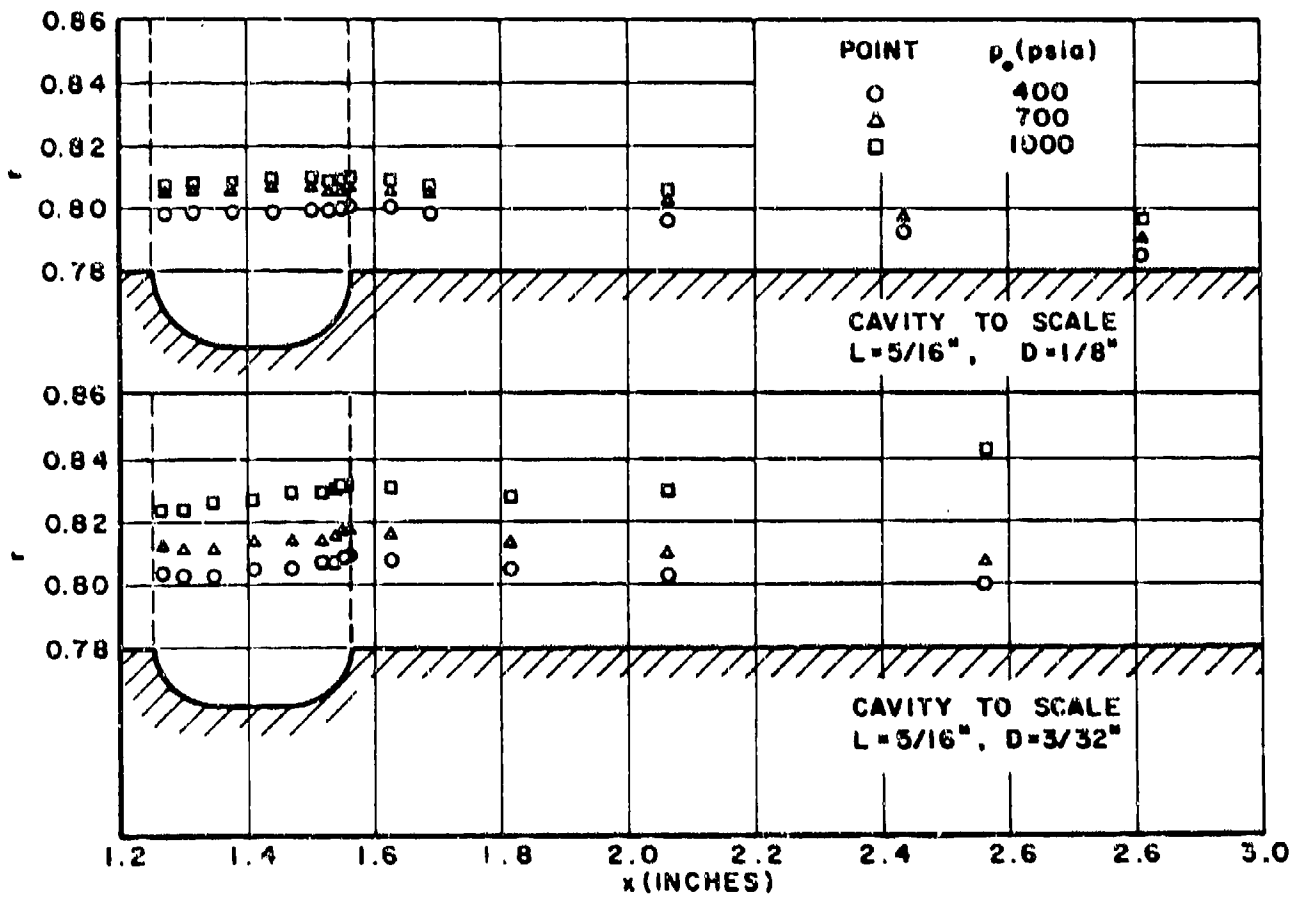


Figure 6. Recovery factor on cavity models

FIG 5-7

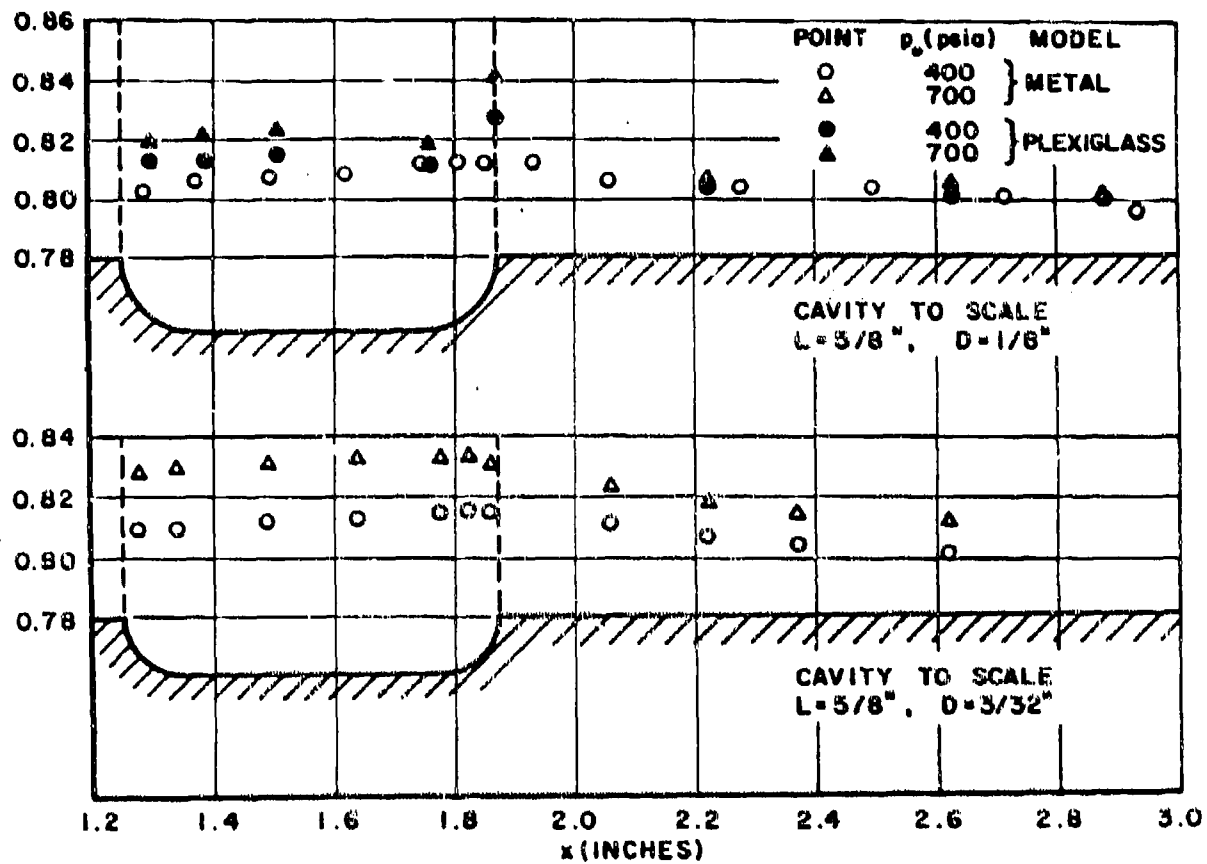


Figure 7. Recovery factor on cavity models

XII 3-3

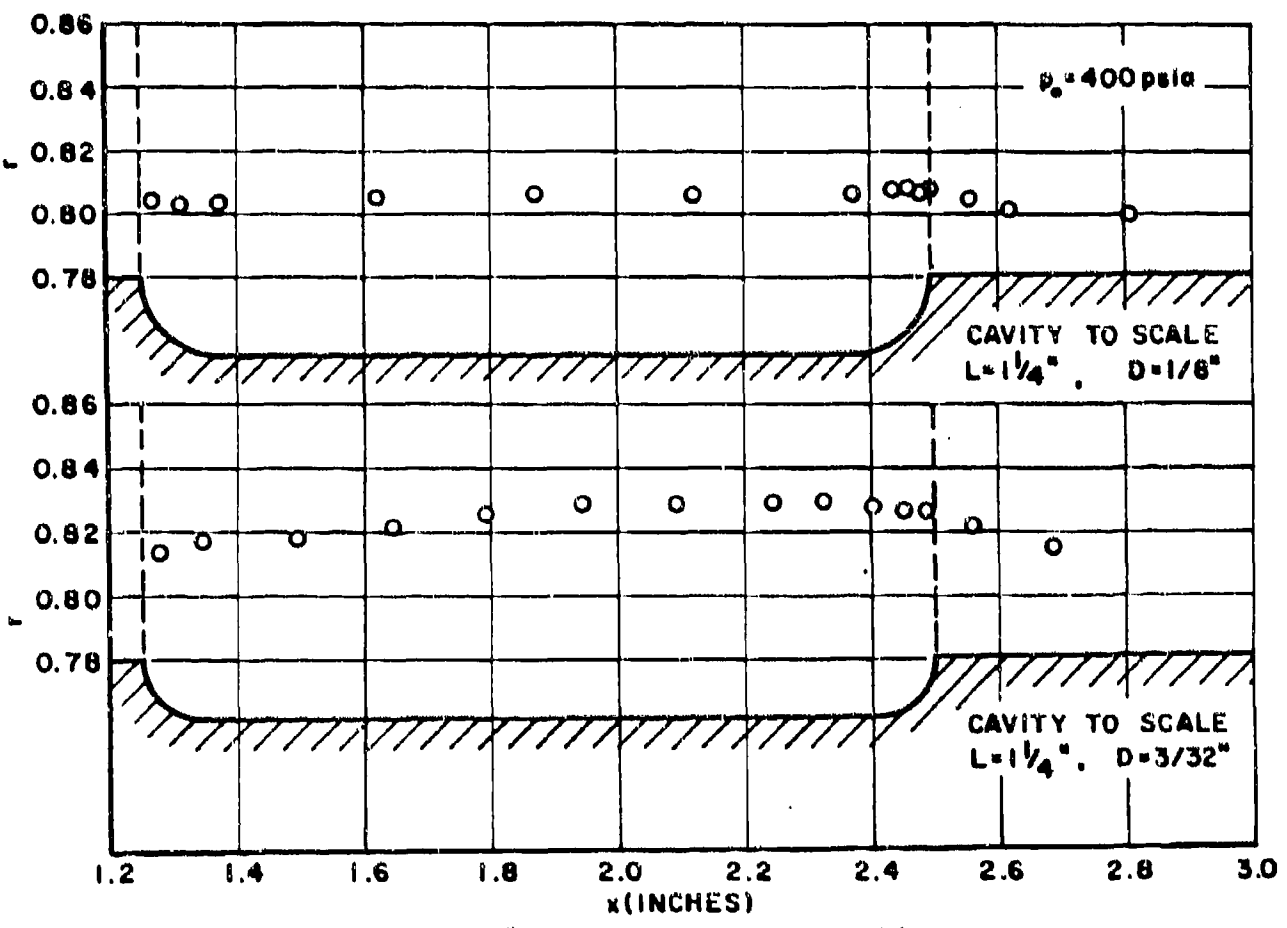


Figure 8. Recovery factor on cavity model

Case III

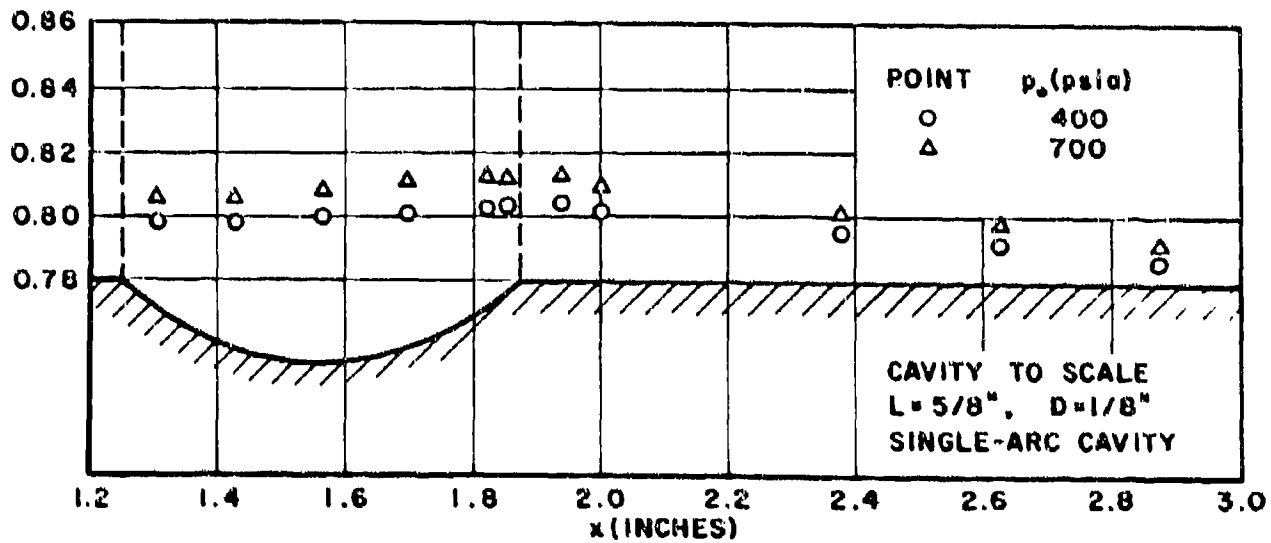


Figure 9. Recovery factor on cavity models

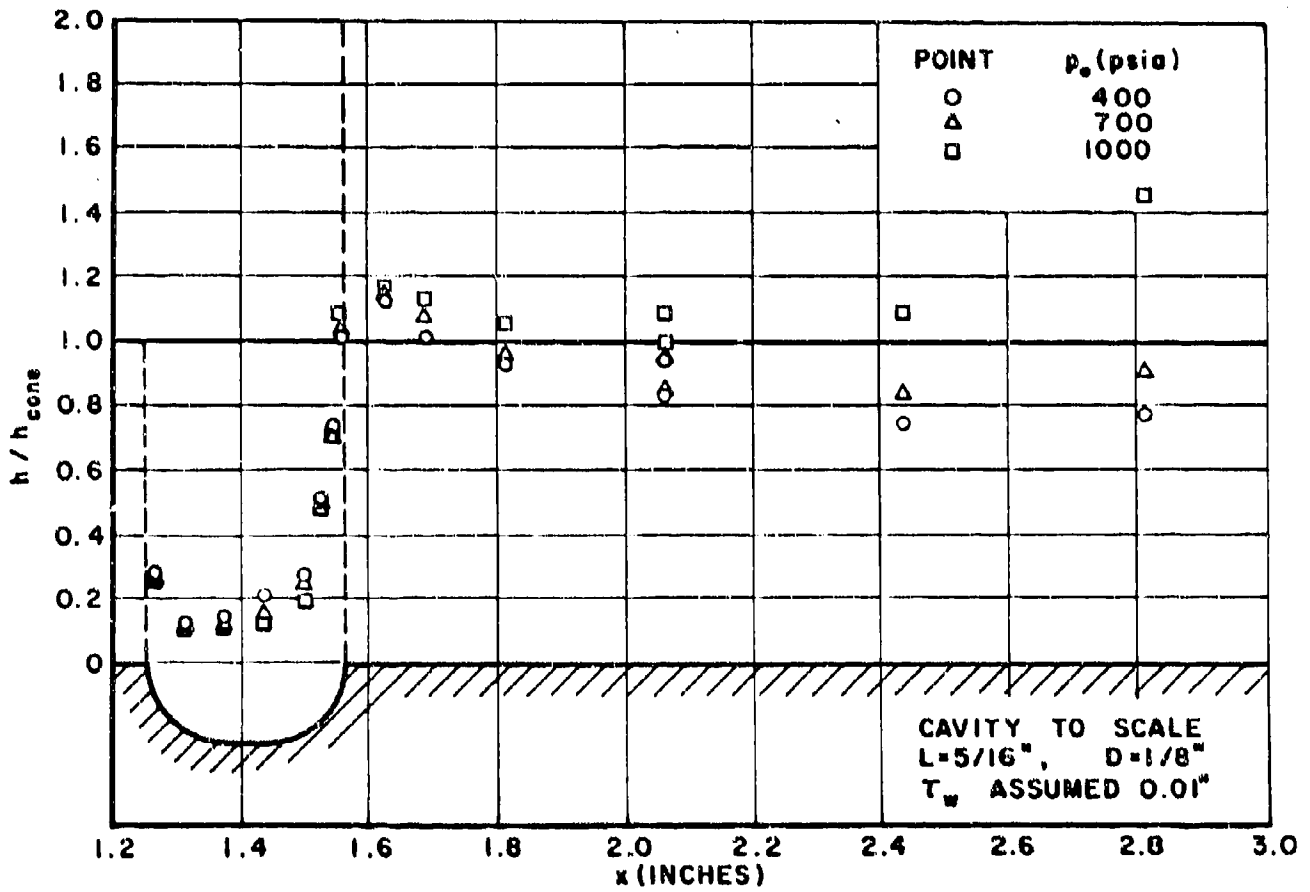


Figure 10. Heat-transfer coefficient on cavity models

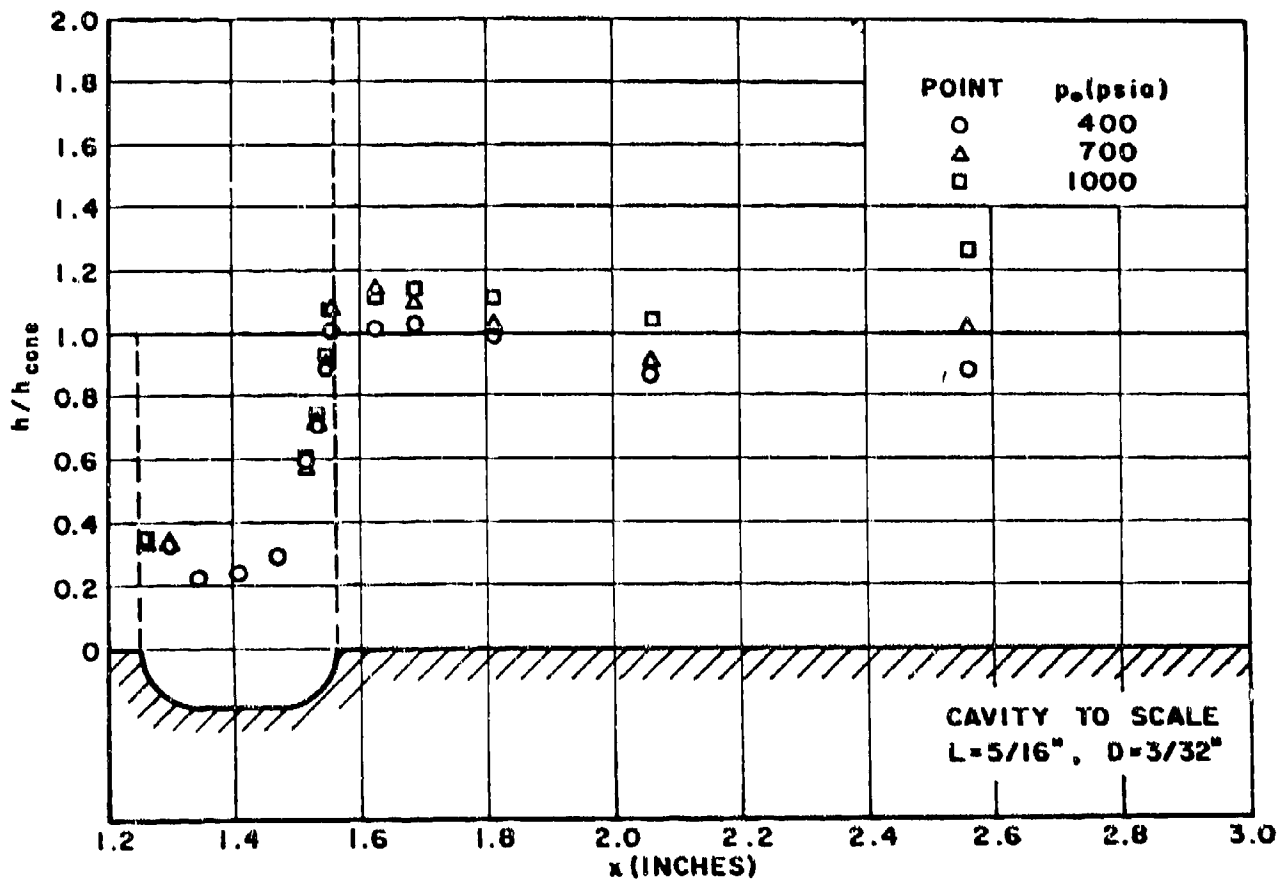


Figure 11. Heat-transfer coefficient on cavity models

XII 34-12

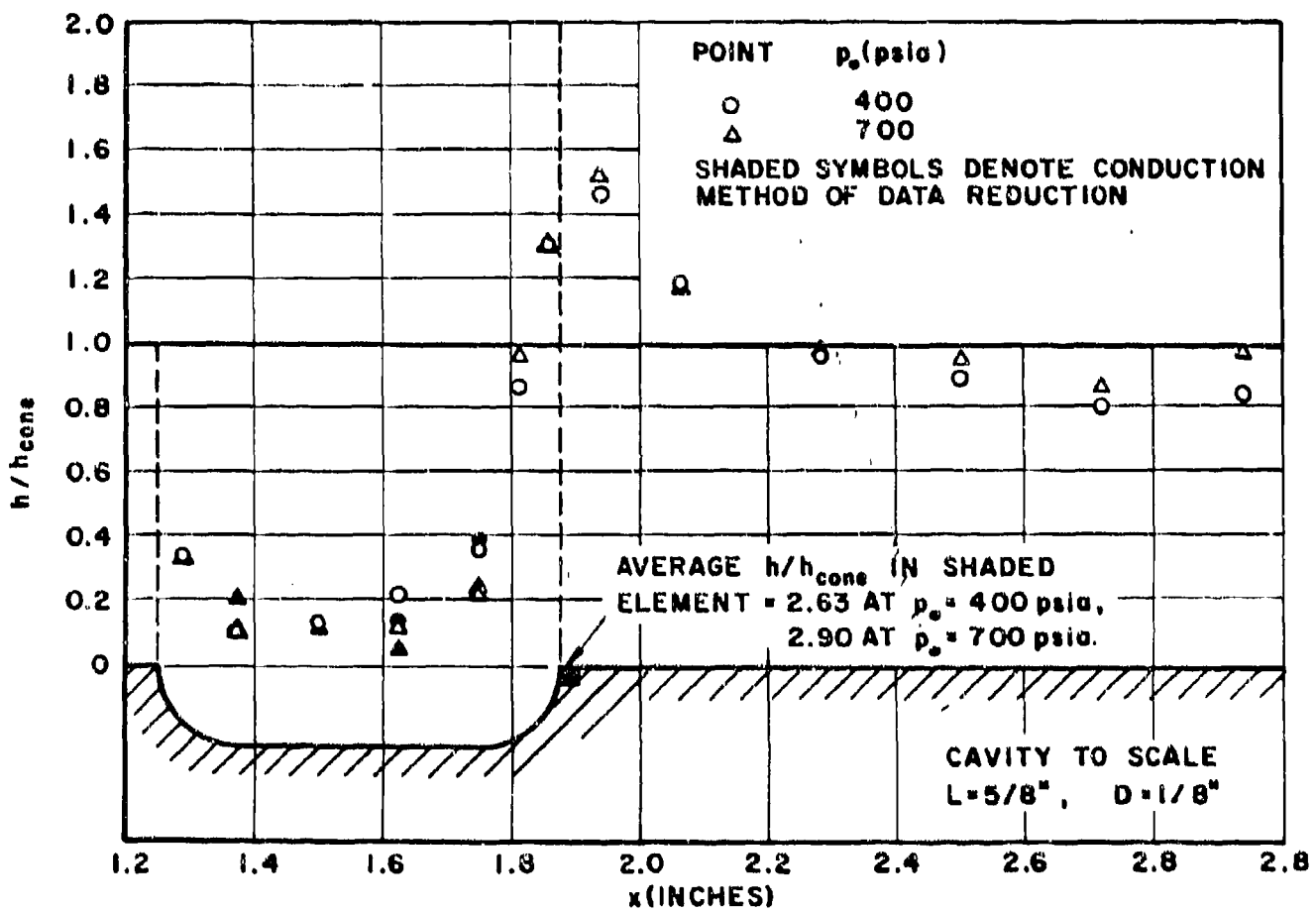


Figure 12. Heat-transfer coefficient on cavity models

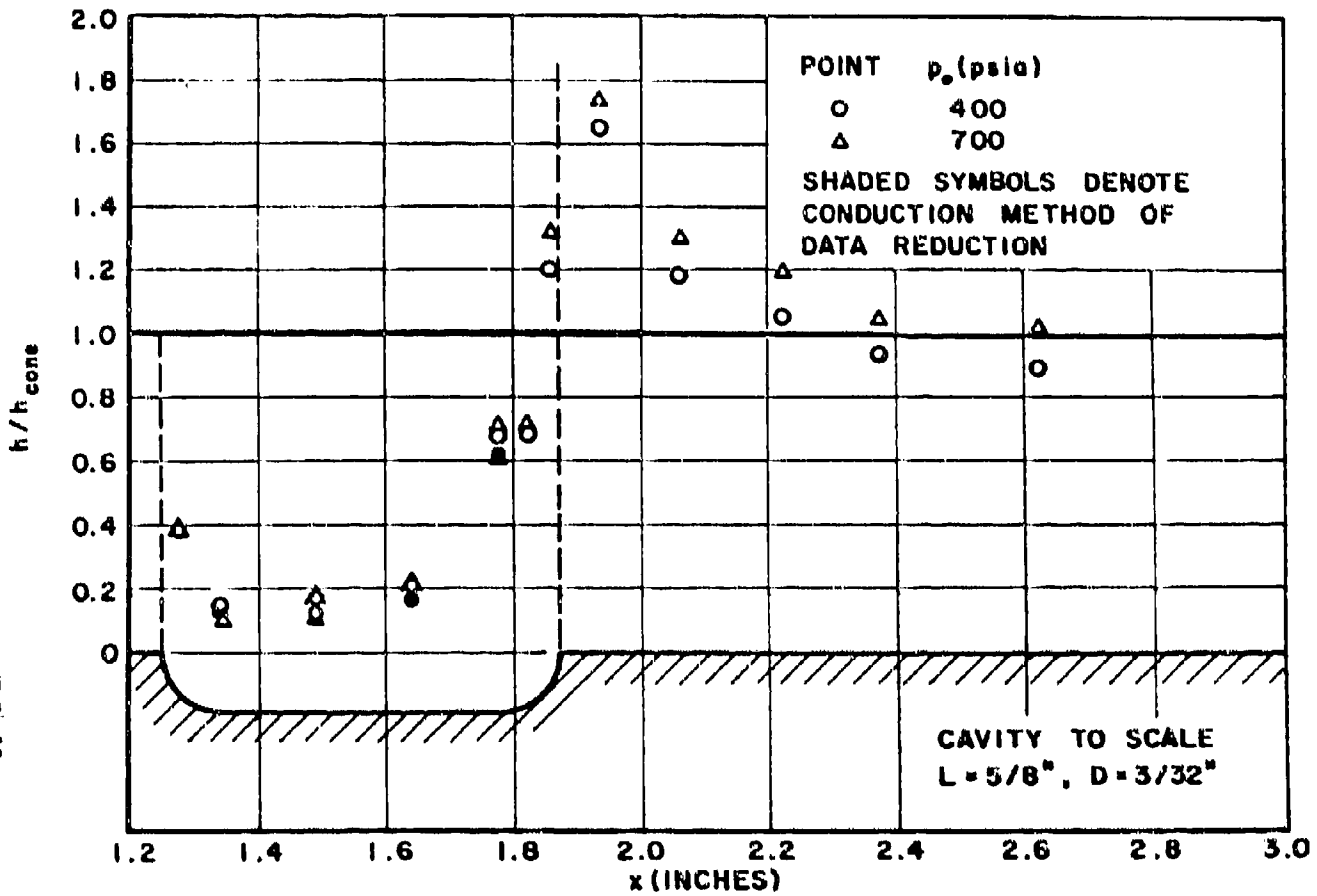


Figure 13. Heat-transfer coefficient on cavity models

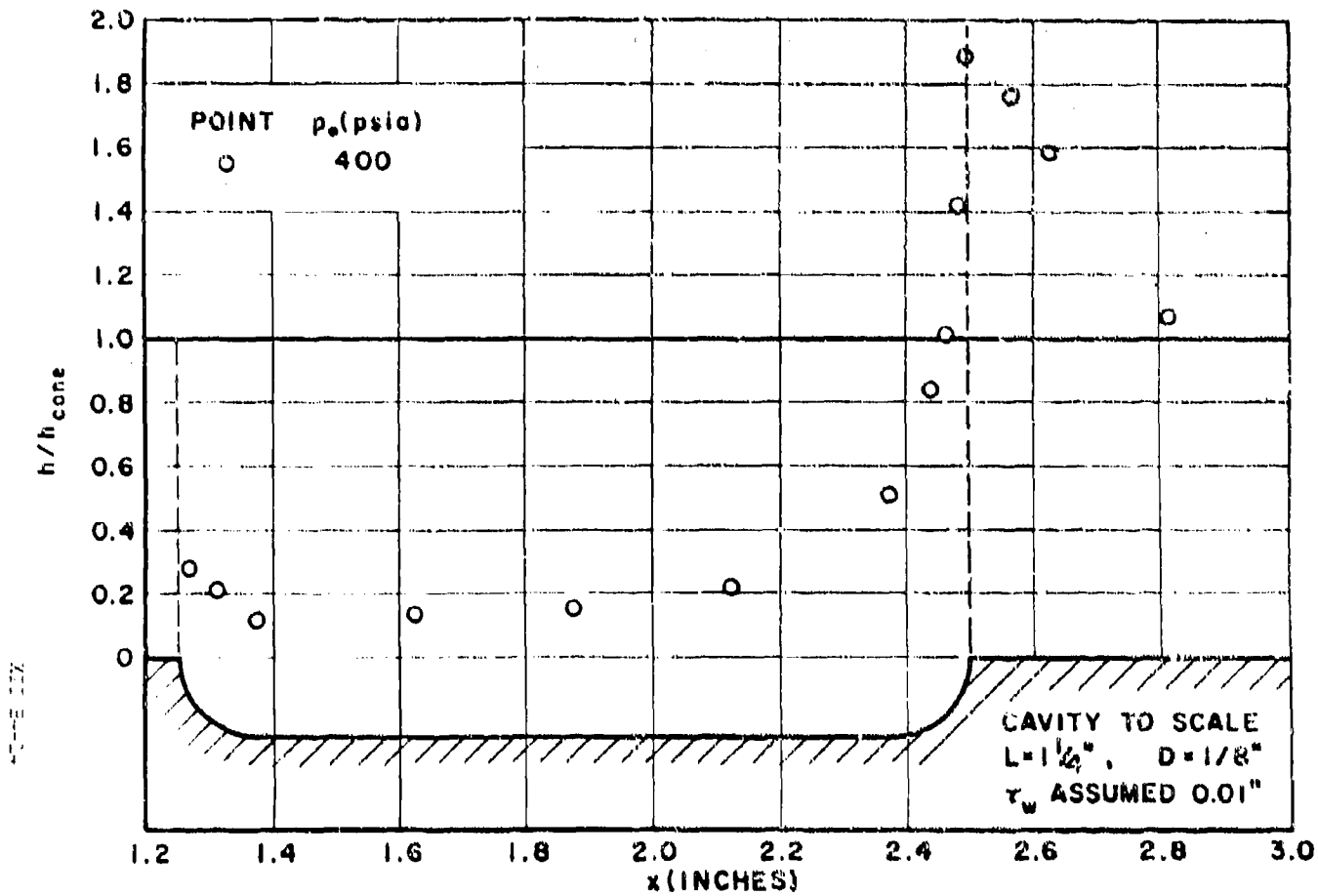


Figure 14. Heat-transfer coefficient on cavity model.

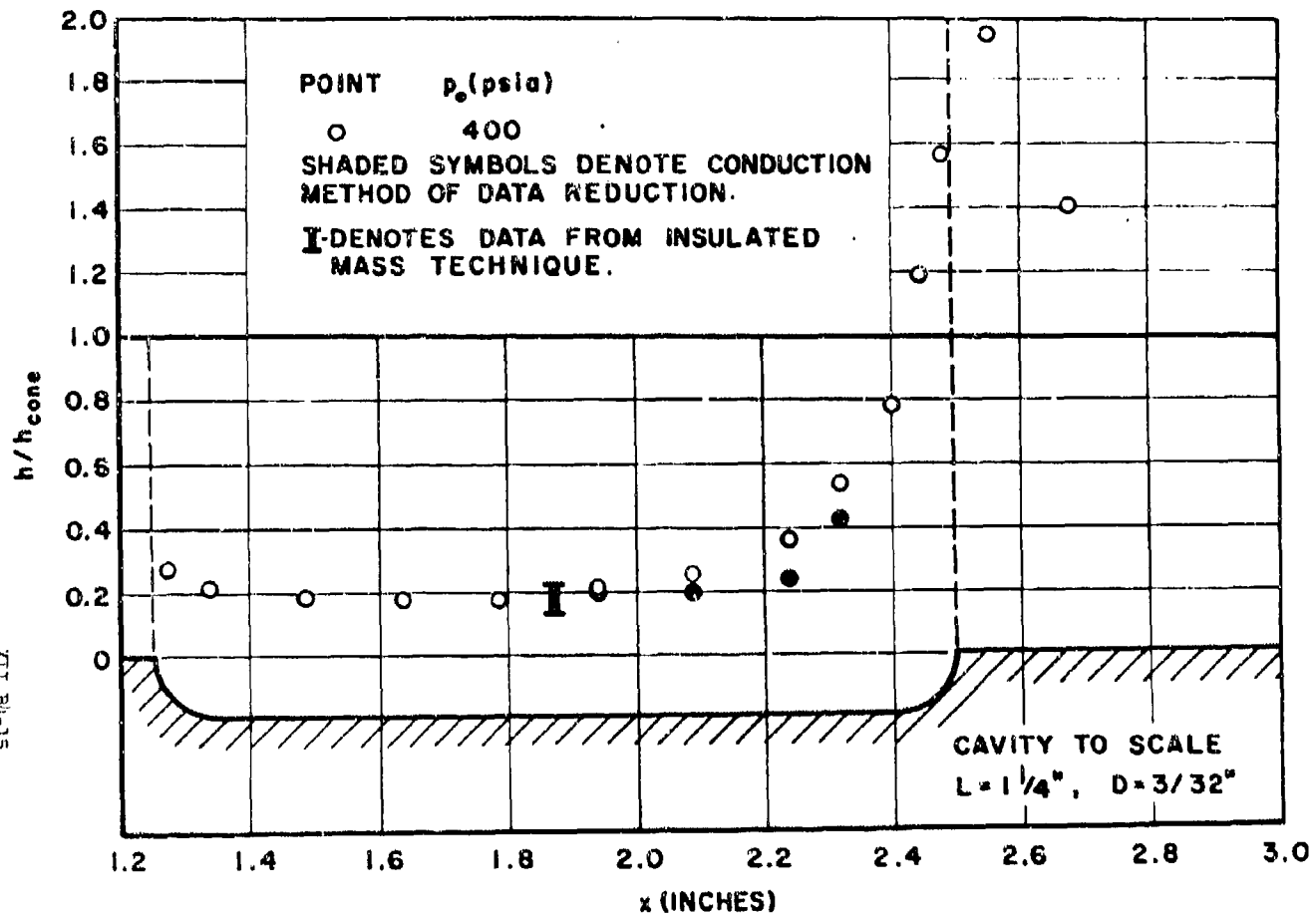


Figure 15. Heat-transfer coefficient on cavity models

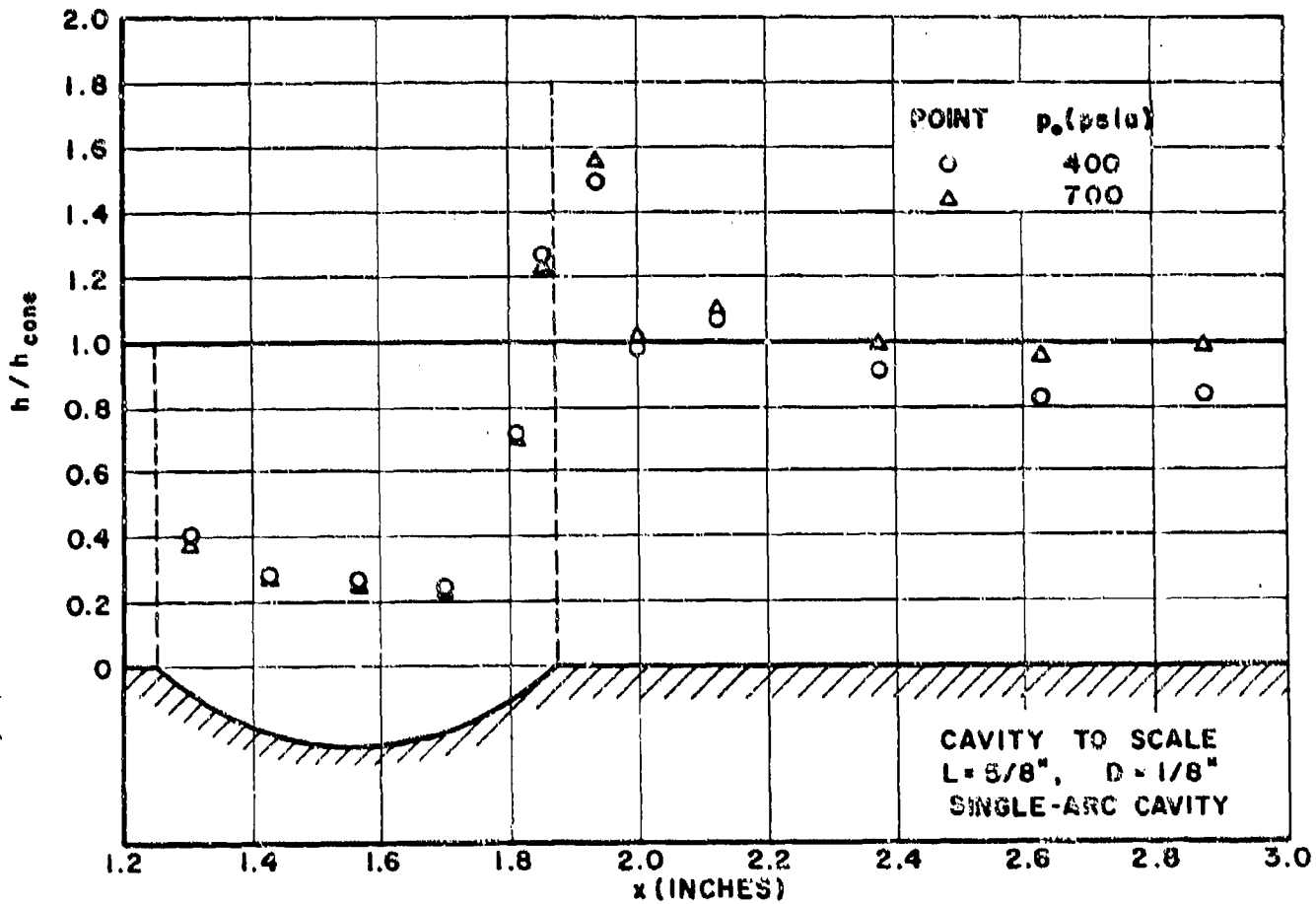
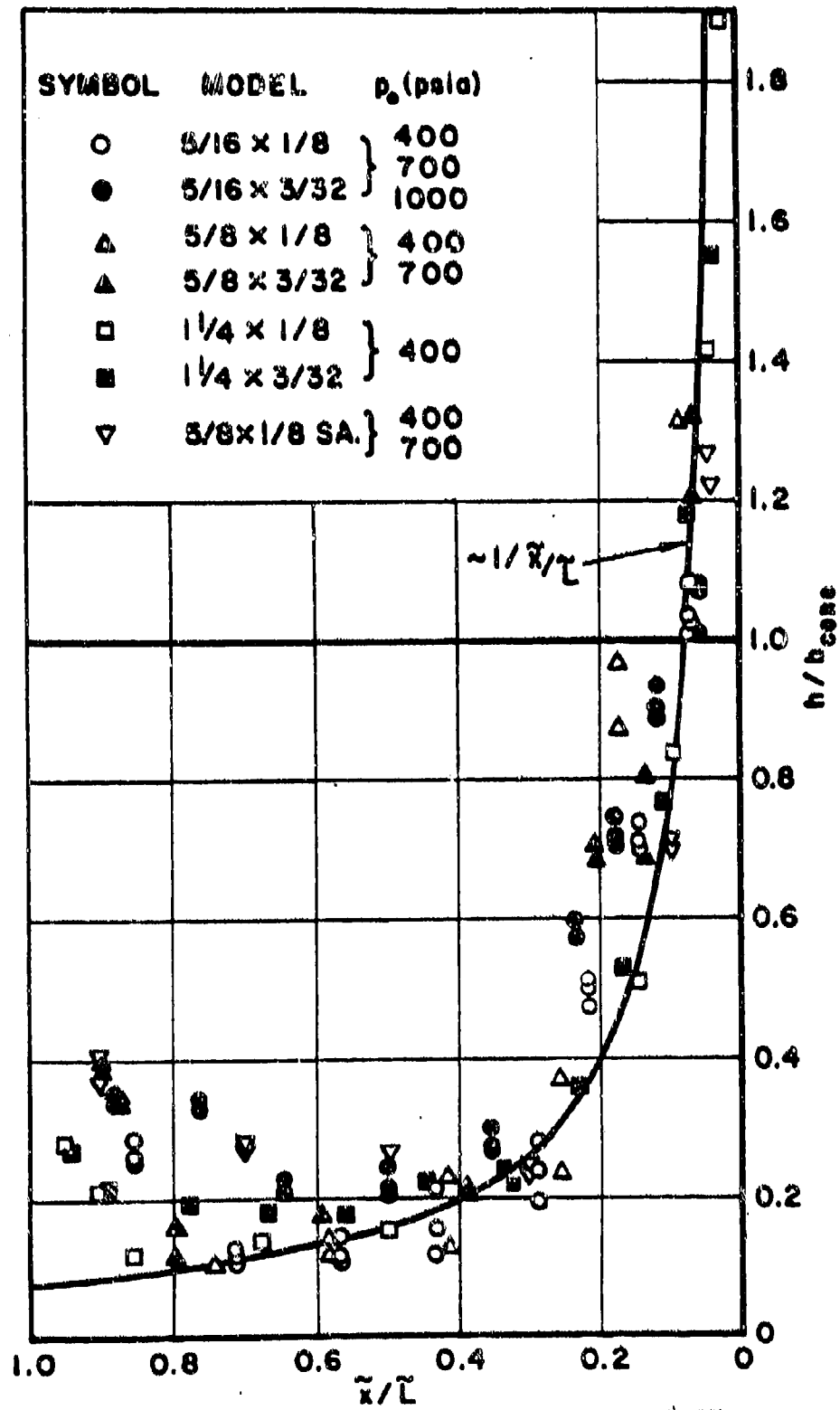


Figure 16. Heat-transfer coefficient on cavity models



XII B4-17

Figure 17. Cavity heat-transfer rates -
all experiments